EBioMedicine 34 (2018) 76–84

Contents lists available at ScienceDirect

EBioMedicine

journal homepage: www.ebiomedicine.com

EBioMedicine
Published by THE LANCET

Research Paper

Development and Validation of an MRI-Based Radiomics Signature for the Preoperative Prediction of Lymph Node Metastasis in Bladder Cancer

Shaoxu Wu [a,1], Junjiong Zheng [a,1], Yong Li [b,1], Zhuo Wu [b], Siya Shi [b], Ming Huang [a], Hao Yu [a], Wen Dong [a], Jian Huang [a,2], Tianxin Lin [a,c,*,2]

[a] Department of Urology, Sun Yat-Sen Memorial Hospital, Sun Yat-Sen University, Guangdong Provincial Key Laboratory of Malignant Tumor Epigenetics and Gene Regulation, Guangzhou, PR China
[b] Department of Radiology, Sun Yat-Sen Memorial Hospital, Sun Yat-Sen University, Guangzhou, PR China
[c] State Key Laboratory of Oncology in South China, PR China

ARTICLE INFO

Article history:
Received 31 May 2018
Received in revised form 4 July 2018
Accepted 19 July 2018
Available online 2 August 2018

Keywords:
Urinary bladder neoplasms
Lymphatic metastasis
Radiomics
Nomogram

ABSTRACT

Background: Preoperative lymph node (LN) status is important for the treatment of bladder cancer (BCa). However, a proportion of patients are at high risk for inaccurate clinical nodal staging by current methods. Here, we report an accurate magnetic resonance imaging (MRI)-based radiomics signature for the individual preoperative prediction of LN metastasis in BCa.

Methods: In total, 103 eligible BCa patients were divided into a training set ($n = 69$) and a validation set ($n = 34$). And 718 radiomics features were extracted from the cancerous volumes of interest (VOIs) on T2-weighted MRI images. A radiomics signature was constructed using the least absolute shrinkage and selection operator (LASSO) algorithm in the training set, whose performance was assessed and then validated in the validation set. Stratified analyses were also performed. Based on the multivariable logistic regression analysis, a radiomics nomogram was developed incorporating the radiomics signature and selected clinical predictors. Discrimination, calibration and clinical usefulness of the nomogram were assessed.

Findings: Consisting of 9 selected features, the radiomics signature showed a favorable discriminatory ability in the training set with an AUC of 0.9005, which was confirmed in the validation set with an AUC of 0.8447. Encouragingly, the radiomics signature also showed good discrimination in the MRI-reported LN negative (cN0) subgroup (AUC, 0.8406). The nomogram, consisting of the radiomics signature and the MRI-reported LN status, showed good calibration and discrimination in the training and validation sets (AUC, 0.9118 and 0.8902, respectively). The decision curve analysis indicated that the nomogram was clinically useful.

Interpretation: The MRI-based radiomics nomogram has the potential to be used as a non-invasive tool for individualized preoperative prediction of LN metastasis in BCa. External validation is further required prior to clinical implementation.

* Corresponding author at: Department of Urology, Sun Yat-sen Memorial Hospital, Sun Yat-sen University, 107 Yan Jiang West Road, Guangzhou, PR China.
E-mail address: lintx@mail.sysu.edu.cn (T. Lin).
[1] Co-first authors.
[2] Co-corresponding authors.

https://doi.org/10.1016/j.ebiom.2018.07.029

Research in Context

Preoperative lymph node (LN) status is important for the treatment of bladder cancer (BCa). However, a proportion of patients are at high risk for inaccurate clinical nodal staging by current methods. Radiomics, the high-throughput extraction of immense volumes of quantitative image features from standard-of-care medical imaging that can be excavated and applied within disease detection, diagnosis, prognostic evaluation, and prediction of the treatment response, has drawn increased attention in cancer research in recent years. We have reported a radiomics study recently, which developed a CT-based radiomics nomogram with favorable discrimination and calibration for the preoperative prediction of LN metastasis in patients with BCa. Since a proportion of BCa patients are diagnosed clinically via MRI, whether the radiomics features extracted from MRI images can be used for LN metastasis prediction in BCa patients is an interesting problem that warrants investigation. However, there has been no study that has determined whether a radiomics signature extracted from MRI images would be capable to preoperatively predict LN metastasis in BCa to date. In this study, we developed and validated an MRI-based radiomics signature for preoperatively predicting LN metastasis in BCa patients, which showed good discrimination in the training and validation sets. Encouragingly, it also performed well in the MRI-reported LN-negative (cN0) subgroup. Our signature demonstrates that radiomics features extracted from MRI images can be used for LN metastasis prediction in BCa patients. The nomogram, incorporating the radiomics signature and MRI-reported LN status, showed favorable discrimination and calibration, providing a non-invasive preoperative prediction tool to identify BCa patients with a high risk of LN metastasis, which may aid in clinical decision-making.

1. Introduction

Bladder cancer (BCa) is the ninth most common cancer and ranks thirteenth as a cause of cancer-related death worldwide [1]. Lymph nodes (LNs) are a common site of metastatic spread in patients with BCa, as approximately 25–30% of BCa patients who undergo radical cystectomy (RC) and pelvic lymph node dissection (PLND) harbor LN metastases [2–8]. LN metastasis is a negative prognostic factor in BCa patients [9–11]. Thus, accurate prediction of LN metastasis in patients with BCa can improve medical decision-making. Magnetic resonance imaging (MRI) and computed tomography (CT) are recommended for preoperative nodal staging in BCa patients in clinical practice. Both MRI and CT detect malignant LN mainly based on their size. However, normal-sized or minimally enlarged LNs assume a considerable proportion of malignant LNs of BCa patients. Such diagnosis pattern leads to understaging patients with small nodal metastases. Therefore, the sensitivity of CT or MRI for detecting malignant LNs is relatively low (31–45%), which has consequently led to a proportion of patients being understaged [12–15].

Radiomics, the high-throughput extraction of immense volumes of quantitative image features from standard-of-care medical imaging that can be excavated and applied within disease detection, diagnosis, prognostic evaluation, and prediction of the treatment response, has drawn increased attention in cancer research in recent years [16, 17]. Radiomics-based signatures have been developed for precision diagnosis and treatment, which may serve as a novel and powerful tool in modern precision medicine [16]. An MRI-based radiomics study has demonstrated that radiomics features extracted from MRI images can be used to distinguish tumor grade in BCa [18]. However, to our knowledge, there has been no study that has determined whether a radiomics signature extracted from MRI images would be capable to preoperatively predict LN metastasis in BCa to date. Recently, we reported a CT-based radiomics study, which developed a radiomics nomogram with favorable discrimination and calibration for the preoperative prediction of LN metastasis in patients with BCa [19]. Since a proportion of BCa patients are diagnosed clinically via MRI, whether the radiomics features extracted from MRI images can be used for LN metastasis prediction in BCa patients is an interesting problem that warrants investigation.

Therefore, the aim of this study was to construct and validate an MRI-based radiomics signature for the preoperative prediction of LN metastasis in patients with BCa. Moreover, we developed an inclusive nomogram that incorporated the radiomics signature and clinical risk factors for providing an individual, preoperative assessment of the risk of LN metastasis in BCa patients.

2. Materials and Methods

2.1. Patients

Ethical approval was obtained from the institutional review board for this retrospective analysis. A total of 103 consecutive BCa patients treated between August 2010 and April 2018 were enrolled in this study according to the specified inclusion and exclusion criteria. Inclusion criteria consisted of the following: (a) BCa patients with pathologically confirmed urothelial carcinoma; (b) laparoscopic RC and extended PLND performed; and (c) standard pelvic MRI performed <20 days before surgery. Exclusion criteria included the following: (a) neoadjuvant chemotherapy or preoperative radiotherapy performed; (b) other tumor diseases occurring at the same period; and (c) have imaging artifacts in the MRI images. The patient recruitment pathway is presented in Supplementary Fig. S1. All enrolled patients were divided into two independent data sets: 69 patients treated between August 2010 and July 2016 were assigned to the training set, whereas 34 patients treated between August 2016 and April 2018 were assigned to the validation set.

Baseline clinical data (age and sex) and pathologic N stage were derived from the medical records. MRI data, including the size of the largest tumor, the number of tumors, T stage and LN status, were recorded by two radiologists with 15 (Yong Li) and 10 years (Zhuo Wu) of experience in pelvic MRI interpretation after reviewing all of the MRI scans. Any disagreement was resolved by a consultation. Note that those patients with pelvic LN > 8 mm or abdominal LN > 10 mm in the maximal short-axis diameter on MRI scans were regarded as clinically LN-positive (cN1-3) [20]. Tumor pathologic staging was performed on the basis of the UICC 7th edition TNM staging system [21].

2.2. Imaging Acquisition, Volumes-of-Interest Segmentation and Radiomic Feature Extraction

Fig. 1 shows the radiomics workflow. All patients underwent pelvic MRI with a 3.0 T MR scanner (Intera Achieva, Philips Medical Systems, Best, the Netherlands). On T2-weighted (T2-w) MR images, urine has a high signal intensity, which allows the bladder tumor margins to be delineated more accurately. Thus, axial T2-w Digital Imaging and Communications in Medicine (DICOM) images were retrieved for radiomics feature extraction. The T2-w image acquisition parameters were as follows: repetition/echo time, 3500-4200/100–120 msec; slice thickness, 4 mm; and spacing, 0.5 mm. Regions of interest (ROIs) of bladder tumors were segmented slice-by-slice using the publicly available 3D Slicer software version 4.7.0. Then, the corresponding ROIs were stacked up to construct volumes of interest (VOIs) of the bladder tumor. More information about the segmentation procedure is shown in the Supplementary Methods. A large set of quantitative radiomics features were extracted using the *PyRadiomics* platform implanted in the 3D Slicer software [22]. The features could be divided into four categories:

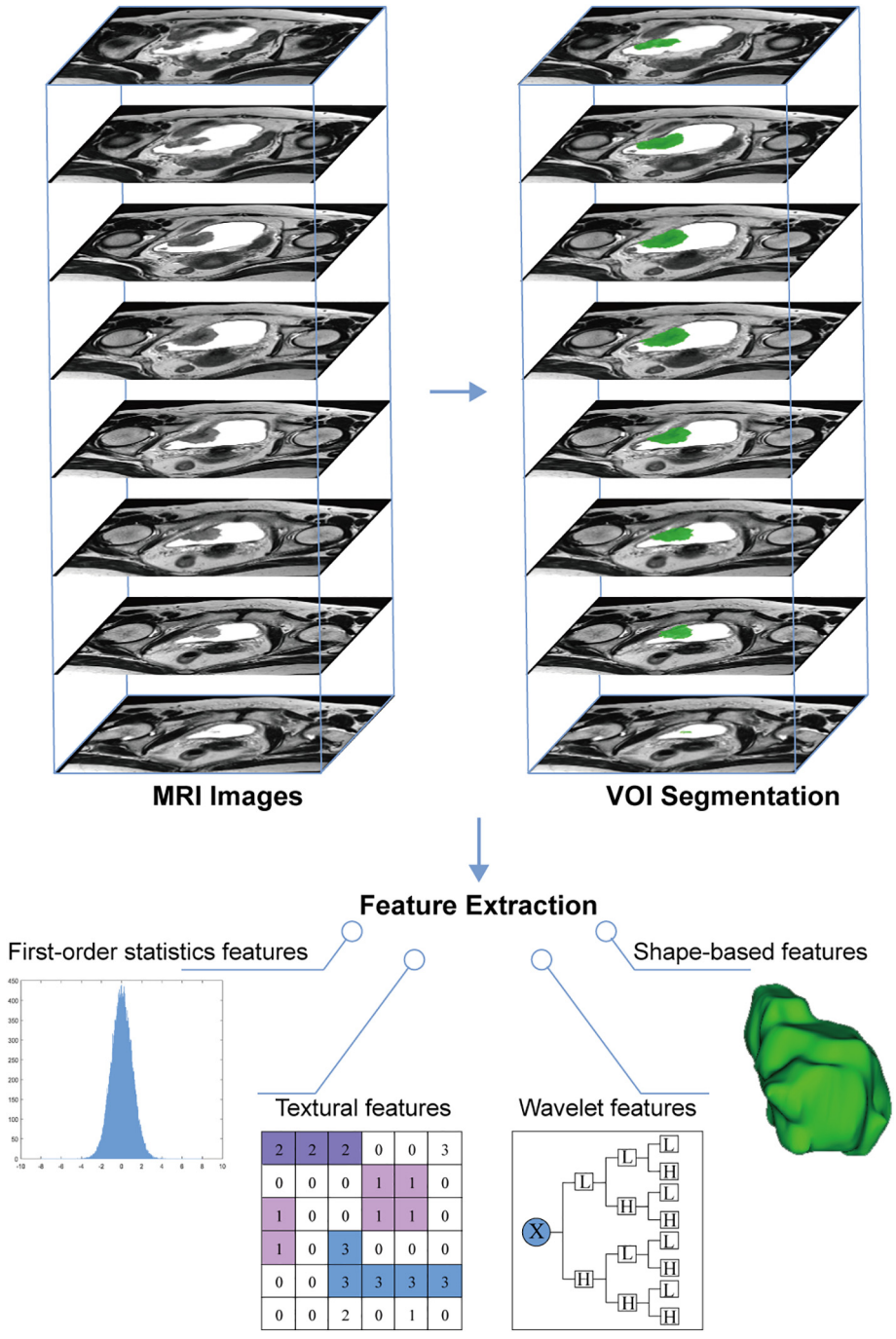

Fig. 1. Radiomics workflow. Firstly, axial T2-w DICOM images are retrieved for radiomics feature extraction. Then, ROIs of bladder tumors are segmented and the corresponding ROIs are stacked up to construct VOI of the bladder tumor. Finally, four categories of radiomics features are extracted from within the defined VOI, including first-order statistics features, shape-based features, textural features, and wavelet features.

(a) first-order statistics features, (b) shape-based features, (c) statistics-based textural features, and (d) wavelet features. The Supplementary Methods and Supplementary Table S2 present more detailed information about the radiomics features and their extraction reproducibility.

2.3. Feature Selection and Radiomics Signature Construction

The least absolute shrinkage and selection operator (LASSO) logistic regression algorithm, a suitable method for the regression of high-dimensional data, was used to select the most significant predictive features from among all the candidate features in the training set [23]. A radiomics signature was constructed using the radiomics score, which was calculated as a linear combination of selected features that were weighted by their respective LASSO coefficients.

2.4. Performance of the Radiomics Signature

The discrimination of the radiomics signature was assessed using the area under the curve (AUC) of the receiver operator characteristic (ROC) in the training set. An optimism-corrected AUC was also calculated by bootstrapping method (2000 bootstrap resamples). Then, the signature was validated in the validation set. Moreover, discrimination of the signature in the MRI-reported LN-negative (cN0) subgroup was also evaluated using the AUC of the ROC in the combined training and validation

set. The Mann–Whitney *U* test was used to assess the potential association of the radiomics score with the LN status in both the training and validation sets. In addition, stratified analyses were also performed in various subgroups in the combined training and validation set.

2.5. Radiomics Nomogram Construction and Performance Assessment

Each candidate predictor including radiomics signature and the clinical candidate predictors (i.e., age, sex, MRI-reported tumor size, MRI-reported number of tumors, MRI-reported T stage and MRI-reported LN status) was tested by using a univariate logistic regression algorithm in the training set. Note that 65 years is widely used as a cutoff for grouping bladder cancer patients in terms of age in clinical practice and research [24, 25]. And 3 cm is used as a cutoff of tumor size for tumor risk categorization according to EAU guidelines for bladder cancer, which is also widely used [26]. Therefore, we used these two cutoffs to group BCa patients in terms of age and MRI-reported tumor size. Variables with $P < 0.2$ on univariate analysis were included in the subsequent multivariate analysis. A multivariate logistic regression algorithm using backward step-wise selection and Akaike's Information Criterion (AIC) was applied to select the significant predictors for prediction model construction. We used the variance inflation factor (VIF) for the collinearity diagnosis of the multivariate logistic regression. Then, a radiomics nomogram was constructed based on the multivariate logistic regression model incorporating the selected predictors.

The discrimination of the radiomics nomogram was assessed with the AUC and the optimism-corrected AUC. The calibration of the radiomics nomogram was assessed with a calibration curve, and the goodness-of-fit of the nomogram was assessed with the Hosmer-Lemeshow test [27].

2.6. Validation of the Radiomics Nomogram

The performance of the radiomics nomogram was validated in the validation set. According to the formula constructed in the training set, a radiomics score was calculated for each patient in the validation set. Then the discrimination and the calibration of the nomogram were assessed using AUC and a calibration curve, and the Hosmer-Lemeshow test were performed. Moreover, ROC analyses were used to compare the discriminatory efficacy of the nomogram to those of the radiomics signature and the selected clinical predictor alone in the combined training and validation set.

2.7. Clinical Usefulness of the Radiomics Nomogram

Decision curve analysis (DCA) was performed to determine the clinical usefulness of the nomogram by calculating the net benefits at different threshold probabilities in the combined training and validation set [28].

2.8. Statistical Analysis

All statistical analyses were implemented using R statistical software version 3.4.2. LASSO logistic regression was performed using the "glmnet" package. The ROC curves were plotted using the "pROC" package. Logistic regression, nomogram construction and calibration plots were performed with the "rms" package. The Hosmer-Lemeshow test was done with the "vcdExtra" package. DCA was performed with the function "dca.R". A two-sided *P* value <0.05 was considered significant.

3. Results

3.1. Patient Clinical Characteristics

Patient characteristics are presented in Table 1 and Supplementary Table S1. Among all 103 BCa patients, 29 (28.2%) developed LN metastasis in this study. According to the subjective MRI-reported LN status, 55.2% (16/29) of the pN1-3 patients were understaged (reported to be cN0), while 6.8% (5/74) of the pN0 patients were overstaged (reported to be cN1-3). No significant difference was found between the training set and the validation set regarding the clinical characteristics (Table 1).

Table 1
Baseline characteristics of the patients.

	Training set (n = 69)	Validation set (n = 34)	*P* value [a]
Sex			
Male	58 (84.1%)	31 (91.2%)	0.493
Female	11 (15.9%)	3 (8.8%)	
Age, years			
<65	45 (65.2%)	20 (58.8%)	0.527
≥65	24 (34.8%)	14 (41.2%)	
MRI-reported tumor size			
≤3 cm	25 (36.2%)	10 (29.4%)	0.492
>3 cm	44 (63.8%)	24 (70.6%)	
MRI-reported number of tumors			
Single	40 (58.0%)	14 (41.2%)	0.109
Multiple	29 (42.0%)	20 (58.8%)	
MRI-reported T stage			
cTa-cT2	31 (44.9%)	16 (47.1%)	0.838
cT3-cT4	38 (55.1%)	18 (52.9%)	
MRI-reported LN status			
cN1–3	11 (15.9%)	7 (20.6%)	0.559
cN0	58 (84.1%)	27 (79.4%)	
Pathologic N stage			
pN1–3	17 (24.6%)	12 (35.3%)	0.258
pN0	52 (75.4%)	22 (64.7%)	

[a] *P* values were obtained from the univariate association analyses between the training and validation set.

3.2. Feature Selection and Radiomics Signature Construction

In total, 718 radiomics features were extracted from each VOI of the bladder tumor on T2-w MR images. Among them, 9 features with non-zero coefficients were selected using the LASSO logistic regression algorithm (Fig. 2a and b). These selected features can be found in the radiomics score calculation formula presented in the Supplementary data.

3.3. Performance of the Radiomics Signature

The radiomics signature showed favorable discrimination with an AUC of 0.9005 (95% CI, 0.8287 to 0.9722, Fig. 2c) in the training set, and the optimism-corrected AUC of the radiomics signature was 0.8872 (95% CI, 0.7827 to 0.9496). This was validated in the validation set with an AUC of 0.8447 (95% CI, 0.6937 to 0.9957, Fig. 2d). The radiomics scores in pN1–3 patients were generally higher than those in pN0 patients. The Mann–Whitney *U* test revealed a significant difference in the radiomics score between pN0 and pN1–3 patients in the training set (median [interquartile range], −1.4085 [−1.8329 to −1.0175] vs. -0.6220 [−0.9711 to −0.0746], respectively, $P < 0.0001$, Fig. 2e), which was confirmed in the validation set (median [interquartile range], −1.1629 [−1.8736 to −1.0013] vs. -0.6175 [−0.9556 to −0.2663], respectively, $P = 0.0006$, Fig. 2f). Significant association between the radiomics score and pathologic LN status was observed when stratified analyses were performed (Supplementary Table S3).

In the combined training and validation set, 18.8% (16/85) cN0 patients were understaged. Therefore, it's important to investigate the discriminatory efficacy of the radiomics signature in the cN0 subgroup. Encouragingly, the radiomics signature also showed good discrimination in the cN0 subgroup (AUC 0.8406, 95% CI, 0.7279 to 0.9533, Fig. 3a). In addition, an optimal radiomics score cutoff value of −1.086

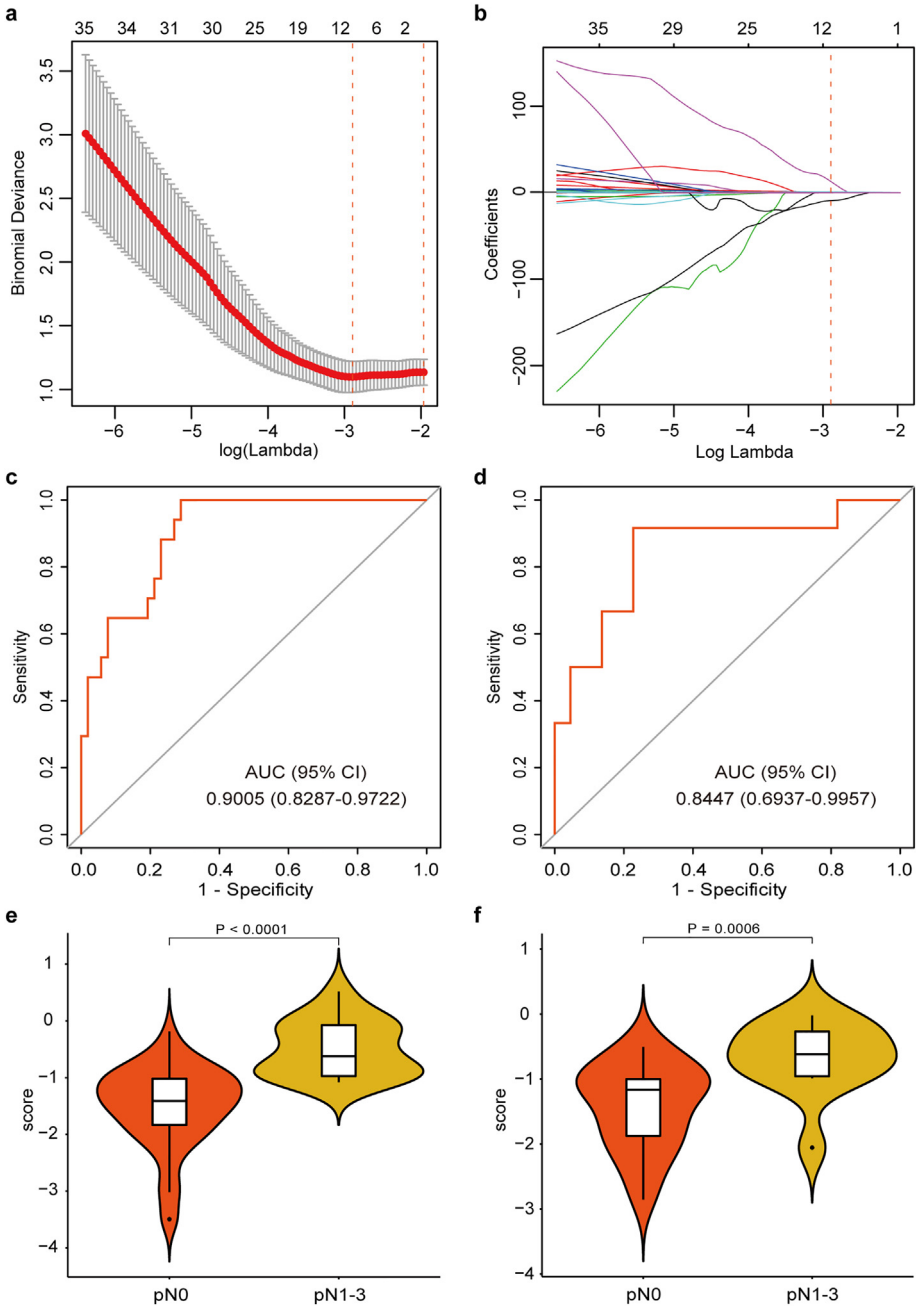

Fig. 2. Texture feature selection using LASSO logistic regression and the performance of the radiomics signature. (a) Selection of the tuning parameter (λ). The LASSO logistic regression model was used with penalty parameter tuning that was conducted by 10-fold cross-validation based on minimum criteria. The binomial deviance was plotted versus log (λ). The dotted vertical lines were plotted at the optimal λ values based on the minimum criteria and 1 standard error of the minimum criteria. The optimal λ value of 0.0553 with log (λ) = −2.895 was selected. (b) LASSO coefficient profiles of the 718 radiomics features. The dotted vertical line was plotted at the λ value of 0.0553, resulting in 9 nonzero coefficients. Plots (c) and (d) present the ROC curves of the radiomics signature in the training and validation sets, respectively. Plots (e) and (f) present the boxplots of the radiomics score in the training and validation sets, respectively.

was defined based on the maximum Youden index in the cN0 subgroup. The waterfall plot for distribution of radiomics score and LN status of individual patients is presented in Fig. 3b, which clearly reveals that almost all patients with LN metastasis (93.8%, 15/16) would avoid being understaged by using the cutoff value of the radiomics signature.

3.4. Radiomics Nomogram Construction and Performance Assessment

Four variables, including the radiomics signature, MRI-reported tumor size, MRI-reported T stage and MRI-reported LN status, were found to be significant at a level of $P < 0.2$ based on the univariate logistic regression algorithm (Table 2). Among them, two predictors, including the radiomics signature and MRI-reported LN status, were selected using the multivariate logistic regression algorithm. After multivariable adjustment by clinical variables, the radiomics score (per 0.2 increase) remained a strong independent predictor for LN metastasis prediction (OR 2.049, 95% CI, 1.453 to 3.335, $P < 0.001$). As for the collinearity diagnosis, the VIFs of the four candidate predictors ranged from 1.0639 to 1.2097, demonstrating that there was no collinearity. Then, a radiomics nomogram incorporating these two predictors was constructed based on the multivariate logistic regression model (Fig. 4a).

The radiomics nomogram yielded an AUC of 0.9118 (95% CI, 0.8433 to 0.9802, Fig. 4b) and an optimism-corrected AUC of 0.8951 (95% CI, 0.7987–0.9553), which indicated that the nomogram had favorable

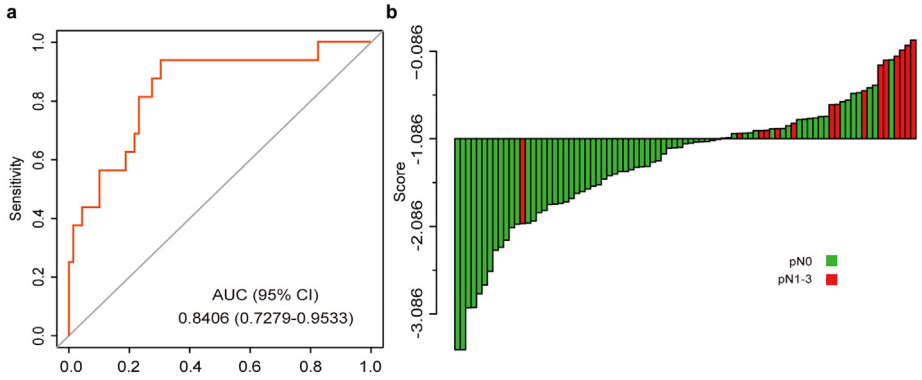

Fig. 3. The predictive performance of the radiomics signature in the cN0 subgroup. (a) ROC curve of the radiomics signature in the cN0 subgroup. (b) Waterfall plot for distribution of radiomics score and pathologically LN status of individual patients. The cutoff value of the radiomics score was −1.086.

discrimination. The calibration curve of the nomogram is presented in Fig. 4d. The Hosmer-Lemeshow test yielded a nonsignificant *P* value of 0.5315, which indicated good calibration power.

3.5. Validation of the Radiomics Nomogram

Good discrimination (Fig. 4c) and good calibration (Fig. 4e) were also observed in the validation set. The AUC of the nomogram was 0.8902 (95% CI, 0.7437 to 1.0000). And the Hosmer-Lemeshow test also yielded a nonsignificant *P* value of 0.1999. Moreover, in the combined training and validation set, the radiomics nomogram achieved better discriminatory efficiency, with the greatest AUC of 0.9007 (95% CI, 0.8299 to 0.9715), compared to either the radiomics signature (AUC 0.8788, 95% CI, 0.8052 to 0.9525) or the MRI-reported LN status alone (AUC 0.6904, 95% CI, 0.5939 to 0.7869, Fig. 5a). Similar findings of model comparisons were also observed in both the training and validation sets (Supplementary Fig. S2).

3.6. Clinical Usefulness of the Radiomics Nomogram

In the DCA, the nomogram offered a net benefit over the "treat-all" or "treat-none" strategy at a threshold probability >3.50% (Fig. 5b), which indicated that the nomogram was clinically useful. For example, with a threshold probability of 40%, use of the radiomics nomogram could provide an added net benefit of 0.1427 compared to the "treat-all" or "treat-none" strategy. Moreover, when DCA performed in both the training and validation sets, similar findings were also observed (Supplementary Fig. S3).

4. Discussion

In the present study, we developed and validated an MRI-based radiomics nomogram incorporating the radiomics signature and the MRI-reported LN status for individualized preoperative prediction of LN metastasis in BCa, which showed favorable discrimination and calibration. Our study demonstrates that radiomics features extracted from MRI images can be used for LN metastasis prediction in BCa patients and provide a non-invasive preoperative prediction tool to identify BCa patients with a high risk of LN metastasis.

LN metastasis in patients with BCa indicates a negative prognosis, with pN1-3 patients showing a significantly lower five-year overall survival rate compared to pN0 patients [5, 9–11]. Thus, preoperative nodal staging is crucial for BCa treatment decision-making. However, the accuracy of the current preoperative nodal staging method is unsatisfactory, with a considerable portion of patients who are understaged or overstaged.

Bilateral PLND combined with RC is considered the standard of care for patients with muscle-invasive bladder cancer (MIBC). Clearly, PLND should be considered an essential part of RC, while the extent of PLND in RC remains a subject of controversy. Previous LN metastasis mapping studies have indicated that a proportion of LN-positive patients have malignant LNs exceeding the region of the standard PLND template [29, 30]. Although no level 1 evidence is available supporting improved outcomes with extended PLND at present, it is reasonable to speculate that a larger PLND template should be performed because it may provide better regional control and more accurate nodal staging [31]. A well-written systematic review also indicated that BCa patients might benefit from extended PLND compared with lesser degrees of dissection [32]. However, extended PLND has not been widely or regularly adopted in current clinical practice, in particular for cN0 patients, because of the higher operative difficulty and the potential increase in perioperative complications.

Neoadjuvant chemotherapy has shown overall survival benefits for BCa patients in individual phase 3 trials and in meta-analyses [33–35]. Even so, a high percentage of patients will not benefit from this approach because of the unsatisfactory response rate. Currently, it is quite difficult to identify those patients who will benefit from neoadjuvant chemotherapy. Therefore, neoadjuvant chemotherapy is performed relatively rarely in clinical practice despite its recommendation by the current guidelines [36, 37]. However, BCa patients with LN metastases are likely to benefit from neoadjuvant chemotherapy because neoadjuvant chemotherapy is conducted to eradicate micrometastatic disease and even malignant LN lesions [38].

Considering the above findings, if clinicians can preoperatively identify patients at high risk of LN metastasis, then such patients might represent an appropriate group for extended PLND and neoadjuvant chemotherapy. Therefore, it is important to develop accurate predictive tools for the preoperative prediction of LN metastasis in BCa patients.

The field of radiomics has developed rapidly in recent years. Radiomics-based tools have been developed to improve diagnostic, prognostic, and predictive accuracy mainly in cancer disease [17]. Recently, we have developed a CT-based radiomics nomogram for the

Table 2
Univariate logistic regression analysis of the radiomics score and clinical candidate predictors in the training set.

Variable	OR (95% CI)	*P**
The radiomics score (per 0.2 increase)	2.118 (1.509–3.450)	< 0.001*
Sex (male vs. female)	0.637 (0.090–2.835)	0.590
Age, years (<65 vs. ≥65)	1.030 (0.311–3.187)	0.959
MRI-reported tumor size (≤3 cm vs. >3 cm)	3.422 (0.972–16.157)	0.077*
MRI-reported number of tumors (single vs. multiple)	0.486 (0.138–1.515)	0.230
MRI-reported T stage (cTa-cT2 vs. cT3-cT4)	2.600 (0.832–9.187)	0.113*
MRI-reported LN status (cN0 vs. cN1-3)	8.400 (2.142–37.626)	0.003*

* $P < 0.2$.

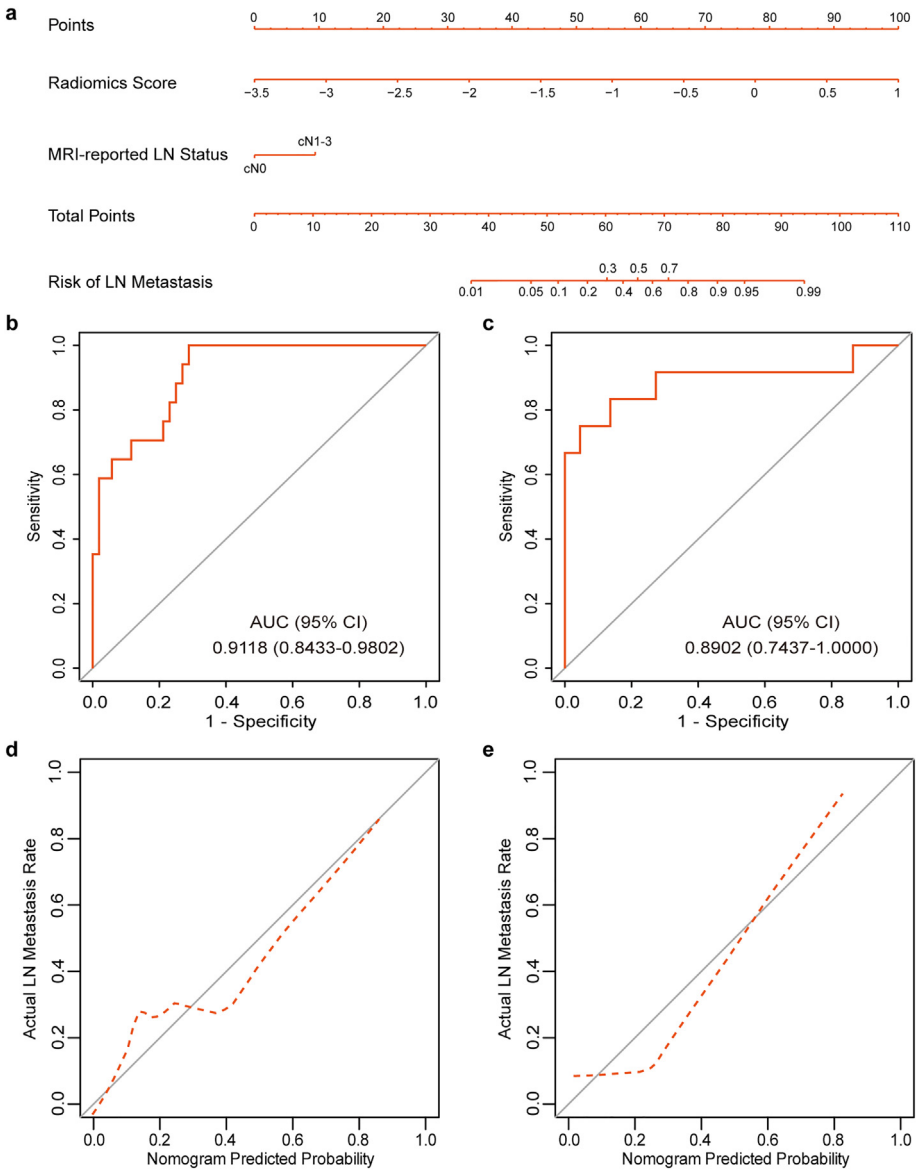

Fig. 4. The MRI-based radiomics nomogram for LN metastasis prediction in patients with BCa. (a) Radiomics nomogram developed for the prediction of LN metastasis. Plots (b) and (c) show the ROC curves of the radiomics nomogram in the training and validation sets, respectively. Plots (d) and (e) present the calibration curves of the nomogram in the training and validation sets, respectively. The calibration curve illustrates the calibration of the nomogram in terms of the agreement between the predicted risk of LN metastasis and the observed outcomes of LN metastasis. The 45° solid grey line represents a perfect prediction, and the dotted red line represents the predictive performance of the nomogram. The dotted line has a closer fit to the solid line, which indicates better predictive accuracy of the nomogram.

preoperative prediction of LN metastasis in patients with BCa [19]. However, in current clinical practices, a proportion of BCa patients are diagnosed clinically using MRI, which is also recommended for preoperative nodal staging in BCa patients. Thus, it is worth discussing whether radiomics features extracted from MRI images can be used for LN metastasis prediction in BCa patients. If possible, an MRI-based radiomics prediction tool should be developed to improve the predictive accuracy of LN metastasis.

Thus, in this study, we attempted to select the most significant predictive features from the radiomics features extracted from MRI images and then to develop an MRI-based radiomics signature. The radiomics signature developed in this study showed good discrimination with AUCs of 0.9005 (95% CI, 0.8287 to 0.9722) in the training set and 0.8447 (95% CI, 0.6937 to 0.9957) in the validation set. Encouragingly, the radiomics signature also showed good discrimination in the cN0 subgroup with an AUC of 0.8406 (95% CI, 0.7279 to 0.9533). Tomography imaging, such as CT and MRI, tends to underestimate the risk of LN metastasis in BCa patients since its sensitivity at detecting malignant LNs is relatively low. Consequently, some patients with BCa diagnosed as cN0 actually harbor LN metastases. Therefore, the precise identification of which cN0 patients will experience LN metastasis is a formidable challenge. Notably, when categorized into low- and high-risk groups according to the optimal radiomics score cutoff value (−1.086) derived from the radiomics signature, the high-risk group (radiomics score > −1.086) showed a greater probability of LN metastasis than the low-risk group, identifying 93.8% (15/16) pN1–3 patients from cN0 patients. Finally, to provide an easy-to-use tool for clinicians, we developed a radiomics nomogram incorporating the radiomics signature and MRI-reported LN status, which showed favorable calibration and discrimination. The performance of the present MRI-based radiomics nomogram is similar to that of our prior CT-based radiomics nomogram in their respective training set (AUC [95% CI], 0.9118 [0.8433 to 0.9802] vs. 0.9262 [0.8657 to 0.9868], respectively) and validation set (AUC [95% CI], 0.8902 [0.7437 to 1.0000] vs. 0.8986 [0.7613 to 0.9901],

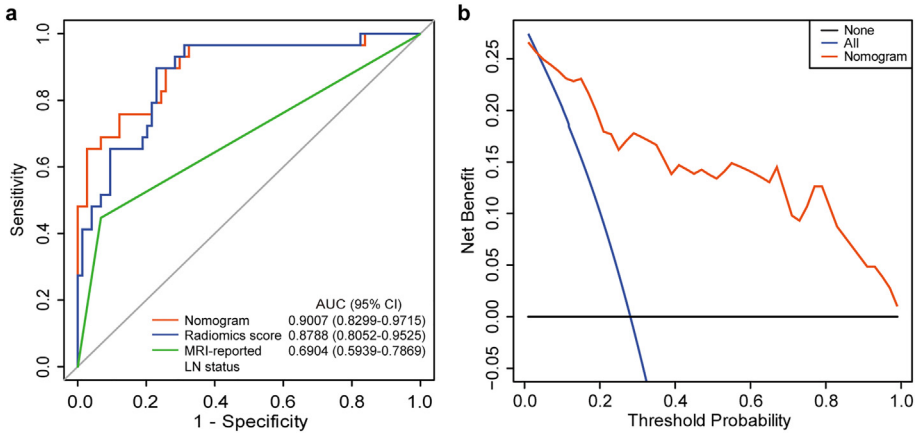

Fig. 5. Model comparisons and clinical usefulness of the radiomics nomogram. (a) ROC curve analyses of the models to compare the predictive performance in all 103 patients. (b) DCA for the nomogram. The net benefit was plotted versus the threshold probability. The red line represents the radiomics nomogram. The blue and black lines represent the hypothesis that all patients and no patients had LN metastases, respectively. The decision curve demonstrates that if the threshold probability is >3.50%, using the radiomics nomogram for LN metastases prediction adds more benefit than treating either all or no patients.

respectively) [19].To our knowledge, a model based only on clinical factors and three genomic classifiers for LN metastasis prediction in BCa patients have been reported, including our recent reported genomic-clinicopathologic nomogram [39–42]. However, this is the first attempt to develop an MRI-based radiomics nomogram for the preoperative prediction of LN metastasis in BCa patients, and this study has several strengths. First, compared to the prior clinical model based only on clinical factors [39], using high-dimensional features in the present study can provide more detailed information about bladder tumor lesion, which contributes to a more accurate prediction model. Second, as regard to the construction of genomic classifier, it may be influenced by the quality of tissue samples related to long storage time or poor storage condition in terms of retrospective design, while the images used for radiomics signature development never degrade since they are stored digitally, thus making the radiomics signature more reliable. Moreover, VOIs (3-dimensional) of bladder tumors were extracted from image slices for radiomics feature extraction rather than the ROIs (2-dimensional) of the bladder tumors, which more effectively revealed the heterogeneity of the entire lesion [43], while only a very small portion of tumor tissue is obtained from the entire lesion when using genomic classifier. Third, the presented MRI-based radiomics nomogram consists of only two items, both of which are available from routine MRI analysis. Thus, our nomogram may serve as a non-invasive tool for the preoperative prediction of LN metastasis in BCa.

Despite its strengths, our study is not devoid of limitations. First, external validation in a larger cohort is needed to confirm the performance of our radiomics nomogram. Second, the ROC analysis for the cN0 subgroup was performed in the combined training and validation set, which might have potential overestimation of the performance of the radiomics signature. The performance of the radiomics model in the cN0 subgroup and the optimal radiomics score cutoff value require further assessment and validation in a larger cohort. Third, the presented nomogram does not include data on genomic classifiers. Although genomic classifiers are promising predictive tools, they still require validation [40, 41]. Thus, further studies are warranted to address this issue.

In conclusion, our study demonstrates the feasibility of applying radiomics features extracted from MRI images for preoperative prediction of LN metastasis in patients with BCa. The presented radiomics nomogram has the potential to be used as a non-invasive tool for individualized preoperative prediction of LN metastasis in BCa with favorable predictive accuracy, especially for cN0 patients. Further external validation is warranted to determine the performance of the nomogram before implementing it in clinical practice.

Funding Sources

This work was funded by Natural Science Foundation of China (81572514, U1301221, 81472384, 81402106, 81372729, 81272808), Natural Science Foundation of Guangdong, China (2016A030313244), Grant [2013]163 from Key Laboratory of Malignant Tumor Molecular Mechanism and Translational Medicine of Guangzhou Bureau of Science and Information Technology, Grant KLB09001 from the Key Laboratory of Malignant Tumor Gene Regulation and Target Therapy of Guangdong Higher Education Institutes, and Grant from Guangdong Science and Technology Department (2015B050501004, 2017B020227007).

Declaration of Interests

We declare that we have no conflicts of interest.

Author Contributions

S.X. Wu, J.J. Zheng and Y. Li contributed equally to this work. Study design: T.X. Lin, J. Huang, S.X. Wu, J.J. Zheng. Development of methodology: S.X. Wu, J.J. Zheng, Y. Li. Data collection: S.Y. Shi, M. Huang, H. Yu, W. Dong. Analysis and interpretation of data: S.X. Wu, J.J. Zheng, Y. Li, Z. Wu. Writing of the manuscript: T.X. Lin, J. Huang, S.X. Wu, J.J. Zheng. Review and/or revision of the manuscript: All authors. Study supervision: J. Huang, T.X. Lin.

Appendix A. Supplementary data

Supplementary data to this article can be found online at https://doi.org/10.1016/j.ebiom.2018.07.029.

References

[1] Antoni, S., Ferlay, J., Soerjomataram, I., Znaor, A., Jemal, A., Bray, F., 2017]. Bladder Cancer incidence and mortality: a global overview and recent trends. Eur Urol 71 (1), 96–108.
[2] Leissner, J., Ghoneim, M.A., Abol-Enein, H., et al., 2004]. Extended radical lymphadenectomy in patients with urothelial bladder cancer: results of a prospective multicenter study. J Urol 171 (1), 139–144.
[3] Vazina, A., Dugi, D., Shariat, S.F., Evans, J., Link, R., Lerner, S.P., 2004]. Stage specific lymph node metastasis mapping in radical cystectomy specimens. J Urol 171 (5), 1830–1834.
[4] Jensen, J.B., Ulhoi, B.P., Jensen, K.M., 2012]. Evaluation of different lymph node (LN) variables as prognostic markers in patients undergoing radical cystectomy and extended LN dissection to the level of the inferior mesenteric artery. BJ. Int 109 (3), 388–393.

[5] Stein, J.P., Lieskovsky, G., Cote, R., et al., 2001]. Radical cystectomy in the treatment of invasive bladder cancer: long-term results in 1,054 patients. J Clin Oncol Off J Am Soc Clin Oncol 19 (3), 666–675.
[6] Baltaci, S., Adsan, O., Ugurlu, O., et al., 2011]. Reliability of frozen section examination of obturator lymph nodes and impact on lymph node dissection borders during radical cystectomy: results of a prospective multicentre study by the Turkish Society of Urooncology. BJ. Int 107 (4), 547–553.
[7] Zehnder, P., Studer, U.E., Skinner, E.C., et al., 2011]. Super extended versus extended pelvic lymph node dissection in patients undergoing radical cystectomy for bladder cancer: a comparative study. J Urol 186 (4), 1261–1268.
[8] Abol-Enein, H., Tilki, D., Mosbah, A., et al., 2011]. Does the extent of lymphadenectomy in radical cystectomy for bladder cancer influence disease-free survival? A prospective single-center study. Eur Urol 60 (3), 572–577.
[9] Zehnder, P., Studer, U.E., Daneshmand, S., et al., 2014]. Outcomes of radical cystectomy with extended lymphadenectomy alone in patients with lymph node-positive bladder cancer who are unfit for or who decline adjuvant chemotherapy. BJ. Int 113 (4), 554–560.
[10] Karl, A., Carroll, P.R., Gschwend, J.E., et al., 2009]. The impact of lymphadenectomy and lymph node metastasis on the outcomes of radical cystectomy for bladder cancer. Eur Urol 55 (4), 826–835.
[11] Bassi, P., Ferrante, G.D., Piazza, N., et al., 1999]. Prognostic factors of outcome after radical cystectomy for bladder cancer: a retrospective study of a homogeneous patient cohort. J Urol 161 (5), 1494–1497.
[12] Daneshmand, S., Ahmadi, H., Huynh, L.N., Dobos, N., 2012]. Preoperative staging of invasive bladder cancer with dynamic gadolinium-enhanced magnetic resonance imaging: results from a prospective study. Urology 80 (6), 1313–1318.
[13] Lodde, M., Lacombe, L., Friede, J., Morin, F., Saourine, A., Fradet, Y., 2010]. Evaluation of fluorodeoxyglucose positron-emission tomography with computed tomography for staging of urothelial carcinoma. BJ. Int 106 (5), 658–663.
[14] Goodfellow, H., Viney, Z., Hughes, P., et al., 2014]. Role of fluorodeoxyglucose positron emission tomography (FDG PET)-computed tomography (CT) in the staging of bladder cancer. BJ. Int 114 (3), 389–395.
[15] Baltaci, S., Resorlu, B., Yagci, C., Turkolmez, K., Gogus, C., Beduk, Y., 2008]. Computerized tomography for detecting perivesical infiltration and lymph node metastasis in invasive bladder carcinoma. Urol Int 81 (4), 399–402.
[16] Lambin, P., Leijenaar, R.T.H., Deist, T.M., et al., 2017]. Radiomics: the bridge between medical imaging and personalized medicine. Nat Rev Clin Oncol 14 (12), 749–762.
[17] Gillies, R.J., Kinahan, P.E., Hricak, H., 2016]. Radiomics: images are more than pictures, they are data. Radiology 278 (2), 563–577.
[18] Zhang, X., Xu, X., Tian, Q., et al., 2017]. Radiomics assessment of bladder cancer grade using texture features from diffusion-weighted imaging. J Magn Reson Imaging: JMRI 46 (5), 1281–1288.
[19] Wu, S., Zheng, J., Li, Y., et al., 2017]. A Radiomics nomogram for the preoperative prediction of lymph node metastasis in bladder Cancer. Clin Cancer Res: Off J Am Assoc Cancer Res 23 (22), 6904–6911.
[20] Barentsz, J.O., Engelbrecht, M.R., Witjes, J.A., de la Rosette, J.J., van der Graaf, M., 1999]. MR imaging of the male pelvis. Eur Radiol 9 (9), 1722–1736.
[21] Sobin, L.H., Gospodarowicz, M., Wittekind, C., 2009]. TNM classification of malignant tumors. Wiley-Blackwell, Hoboken.
[22] van Griethuysen, J.J.M., Fedorov, A., Parmar, C., et al., 2017]. Computational radiomics system to decode the radiographic phenotype. Cancer Res 77 (21) [e104-e7].
[23] Tibshirani, R., 1996]. Regression shrinkage and selection via the lasso. J R Stat Soc Ser B (Method) 267–288.
[24] Sylvester, R.J., van der Meijden, A.P., Oosterlinck, W., et al., 2006]. Predicting recurrence and progression in individual patients with stage ta T1 bladder cancer using EORTC risk tables: a combined analysis of 2596 patients from seven EORTC trials. Eur Urol 49 (3) [466-5; discussion 75-7].
[25] Zargar-Shoshtari, K., Zargar, H., Lotan, Y., et al., 2016]. A multi-institutional analysis of outcomes of patients with clinically node positive urothelial bladder Cancer treated with induction chemotherapy and radical cystectomy. J Urol 195 (1), 53–59.
[26] EAU guidelines on non-muscle-invasive bladder cancer. Sect. 7.6. European Association of Urology 2018-06-28. http://uroweb.org/guideline/non-muscle-invasive-bladder-cancer/#7_6.
[27] Kramer, A.A., Zimmerman, J.E., 2007]. Assessing the calibration of mortality benchmarks in critical care: the Hosmer-Lemeshow test revisited. Crit Care Med 35 (9), 2052–2056.
[28] Vickers, A.J., Elkin, E.B., 2006]. Decision curve analysis: a novel method for evaluating prediction models. Med Decis Making: Int J Soc Med Decis Making 26 (6), 565–574.
[29] Dorin, R.P., Daneshmand, S., Eisenberg, M.S., et al., 2011]. Lymph node dissection technique is more important than lymph node count in identifying nodal metastases in radical cystectomy patients: a comparative mapping study. Eur Urol 60 (5), 946–952.
[30] Wang, L., Mudaliar, K., Mehta, V., et al., 2014]. Seeking a standard for adequate pathologic lymph node staging in primary bladder carcinoma. Virchows Archiv: Int J Pathol 464 (5), 595–602.
[31] Kamat, A.M., Hahn, N.M., Efstathiou, J.A., et al., 2016]. Bladder cancer. Lancet (London, England) 388 (10061), 2796–2810.
[32] Bruins, H.M., Veskimae, E., Hernandez, V., et al., 2014]. The impact of the extent of lymphadenectomy on oncologic outcomes in patients undergoing radical cystectomy for bladder cancer: a systematic review. Eur Urol 66 (6), 1065–1077.
[33] Griffiths, G., Hall, R., Sylvester, R., Raghavan, D., Parmar, M.K., 2011]. International phase III trial assessing neoadjuvant cisplatin, methotrexate, and vinblastine chemotherapy for muscle-invasive bladder cancer: long-term results of the BA06 30894 trial. J Clin Oncol Off J Am Soc Clin Oncol 29 (16), 2171–2177.
[34] Advanced Bladder Cancer Meta-Analysis Collaboration, 2005]. Neoadjuvant chemotherapy in invasive bladder cancer: update of a systematic review and meta-analysis of individual patient data advanced bladder cancer (ABC) meta-analysis collaboration. Eur Urol 48 (2), 202–205 [discussion 5-6].
[35] Grossman, H.B., Natale, R.B., Tangen, C.M., et al., 2003]. Neoadjuvant chemotherapy plus cystectomy compared with cystectomy alone for locally advanced bladder cancer. N Engl J Med 349 (9), 859–866.
[36] Martini, T., Gilfrich, C., Mayr, R., et al., 2017]. The use of neoadjuvant chemotherapy in patients with urothelial carcinoma of the bladder: current practice among clinicians. Clin Genitourin Cancer 15 (3), 356–362.
[37] Alfred Witjes, J., Lebret, T., Comperat, E.M., et al., 2017]. Updated 2016 EAU guidelines on muscle-invasive and metastatic bladder Cancer. Eur Urol 71 (3), 462–475.
[38] Mertens, L.S., Meijer, R.P., Meinhardt, W., et al., 2014]. Occult lymph node metastases in patients with carcinoma invading bladder muscle: incidence after neoadjuvant chemotherapy and cystectomy vs after cystectomy alone. BJ. Int 114 (1), 67–74.
[39] Karakiewicz, P.I., Shariat, S.F., Palapattu, G.S., et al., 2006]. Precystectomy nomogram for prediction of advanced bladder cancer stage. Eur Urol 50 (6), 1254–1260 [discussion 61-2].
[40] Smith, S.C., Baras, A.S., Dancik, G., et al., 2011]. A 20-gene model for molecular nodal staging of bladder cancer: development and prospective assessment. Lancet Oncol 12 (2), 137–143.
[41] Seiler, R., Lam, L.L., Erho, N., et al., 2016]. Prediction of lymph node metastasis in patients with bladder Cancer using whole transcriptome gene expression signatures. J Urol 196 (4), 1036–1041.
[42] Wu, S.X., Huang, J., Liu, Z.W., et al., 2018]. A genomic-clinicopathologic nomogram for the preoperative prediction of lymph node metastasis in bladder Cancer. EBioMedicine 31, 54–65.
[43] Lin, W.C., Chen, J.H., 2015]. Pitfalls and limitations of diffusion-weighted magnetic resonance imaging in the diagnosis of urinary bladder Cancer. Trans Oncol 8 (3), 217–230.